IEEE Trans. Signal Processing, vol. 42, no. 9, Sept. 1994, pp. 2513–2520

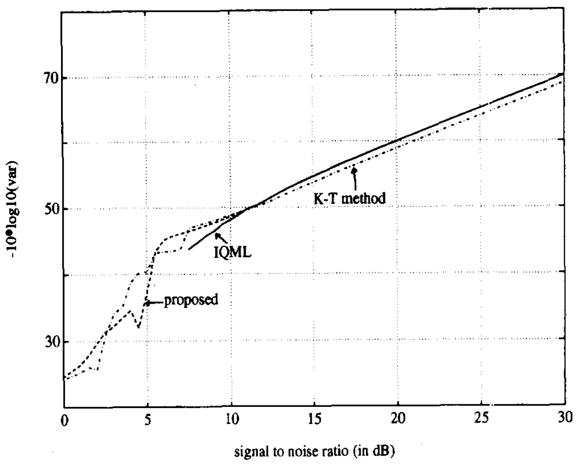

Fig. 6. Estimator variance versus SNR. Example 4: $f = 0.35$.

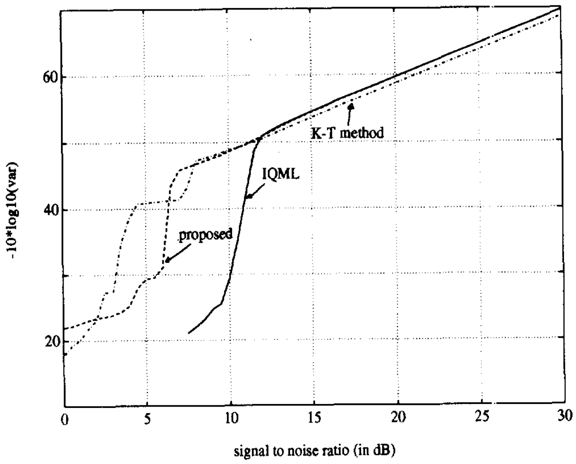

Fig. 7. Estimator variance versus SNR. Example 4: $f = 0.37$.

I is used herein) may alleviate some of these problems. This would be followed by a host of other subjective decisions: deciding whether $\mathrm{Re}\{a[0]\} = 1$ or $\mathrm{Im}\{a[0]\} = 1$ should be chosen, or trying both and deciding which one truly maximizes the likelihood function, or if a local extrema has been reached, etc. Each such proposal would have to be extensively tested to check for reliable performance. Instead, one may choose the other available option, i.e., one of solving (12), which provides a much simpler approach and is theoretically permissible.

III. Conclusion

An invalid constraint in the implementation of the KiSS/IQML algorithm for frequency estimation is pointed out and causes the algorithm to perform poorly for a range of frequency configurations. Better frequency estimators can be had by incorporating a consistent constraint.

References

[1] Y. Bresler and A. Macovski, "Exact maximum likelihood parameter estimation of superimposed exponential signals in noise," *IEEE Trans. Acoust., Speech, Signal Processing,* pp. 1081–1089, Oct. 1986.
[2] P. Comon and G. H. Golub, "Tracking a few extreme singular values and vectors in signal processing," *Proc. IEEE,* pp. 1327–1343, Aug. 1990.
[3] S. M. Kay, *Modern Spectral Estimation.* Englewood Cliffs, NJ: Prentice-Hall, 1988.
[4] R. Kumaresan, L. L. Scharf, and A. K. Shaw, "An algorithm for pole-zero modeling and spectral analysis," *IEEE Trans. Acoust., Speech, Signal Processing,* pp. 637–640, June 1986.
[5] R. Kumaresan and A. K. Shaw, "Superresolution by structured matrix approximation," *IEEE Trans. Antennas Propagat.,* pp. 36–44, Jan. 1988.
[6] S. L. Marple, *Digital Spectral Analysis.* Englewood Cliffs, NJ: Prentice-Hall, 1987.
[7] L. L. Scharf, *Statistical Signal Processing.* Reading, MA: Addison-Wesley, 1990.
[8] A. K. Shaw, "Structured matrix approximation problems in signal processing," Ph.D. dissertation, Univ. of Rhode Island, Kingston, RI, Sept. 1987.
[9] P. Stoica and K. C. Sherman, "Novel eigenanalysis method for direction estimation," *Proc. Inst. Elec. Eng.,* pt. F, pp. 19–26, Feb. 1990.
[10] D. W. Tufts and R. Kumaresan, "Estimation of frequencies of multiple sinusoids: Making linear prediction perform like maximum likelihood," *Proc. IEEE,* pp. 975–989, Sept. 1982.

Time-Frequency Signal Synthesis with Time-Frequency Extrapolation and Don't-Care Regions

Franz Hlawatsch, Antonio H. Costa, and Werner Krattenthaler

***Abstract*—The application of Wigner distribution (WD)-based signal synthesis to signal separation problems is often adversely affected by WD interference terms. We present a modified signal synthesis method where the use of a masked WD allows the definition of don't-care regions. In the don't-care regions, detrimental interference terms (whose time-frequency location is assumed to be known) are ignored. The synthesis result is calculated using a modified version of the quasi power algorithm previously proposed for smoothed WD's. The new synthesis method is shown to possess a desirable time-frequency extrapolation capability as well as a potential tendency to produce spurious signal components in the don't-care regions. The occurrence of spurious signal components can be avoided by the inclusion of an "energy penalty."**

I. Signal Synthesis Using Masked Wigner Distributions

The discrete-time Wigner distribution[1] (WD) [1], [2]

$$W_x(n,\theta) = 2\sum_m c_x(n,m)\, e^{-j4\pi\theta m}$$

Manuscript received April 13, 1992; revised December 27, 1993. This work was supported by the Fonds zur Förderung der wissenschaftlichen Forschung under grants P7354-PHY and J0530-TEC.
F. Hlawatsch is with the Institut für Nachrichtentechnik und Hochfrequenztechnik, Technische Universität Wien, A-1040 Vienna, Austria.
A. H. Costa is with the Department of Electrical Engineering Technology, University of Massachusetts Dartmouth, North Dartmouth, MA 02747 USA.
W. Krattenthaler is with the Forschungszentrum Seibersdorf, A-2444 Seibersdorf, Austria.
IEEE Log Number 9403278.

[1] In (1) and subsequent equations, $x(n)$ is the discrete-time signal under analysis, n is a discrete time index, θ is a normalized frequency, and summations run from $-\infty$ to ∞.

1053-587X/94$04.00 © 1994 IEEE

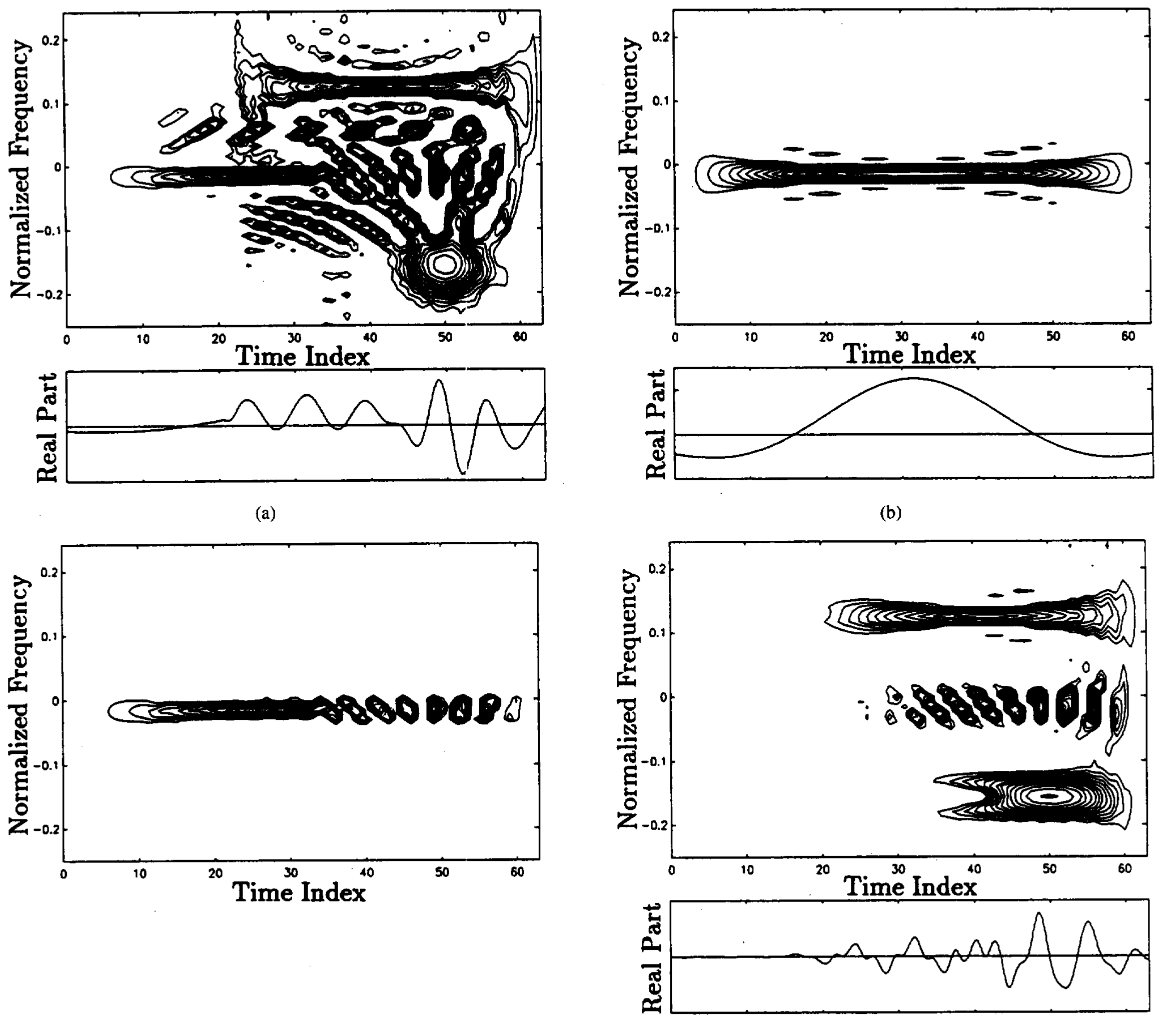

Fig. 1. Application of conventional WD-based signal synthesis to a signal separation problem: (a) Real part and WD of a three-component signal; (b) real part and WD of middle signal component (desired result of signal synthesis); (c) TF model function formed by masking the WD of the three-component signal; (d) result of WD-based synthesis from the model in (c).

$$\text{with} \quad c_x(n,m) = x(n+m)\,x^*(n-m) \tag{1}$$

is a time-frequency (TF) representation that has found widespread application [3]. The WD can be used for a TF implementation of signal processing by modifying a signal's WD and synthesizing a new signal from the modified WD [4]–[7]. However, it has been shown [8] that conventional WD-based signal synthesis is often adversely affected by the WD's cross or interference terms (IT's). An example is considered in Fig. 1. A signal component is to be isolated out of a three-component signal by masking the WD of the overall signal and applying conventional signal synthesis to the masked WD. Unfortunately, the IT of the two other signal components is superimposed on the WD of the desired signal component, which causes the signal synthesis result to be entirely erroneous (see [8] for a mathematical analysis of this situation).

In this correspondence, we are proposing a modified signal synthesis method. We assume that the troublesome IT's are contained in a *known* region D of the TF plane. We first define a *masked WD* (MWD)

$$W_x^{(D)}(n,\theta) \triangleq M_D(n,\theta)\,W_x(n,\theta)$$

$$\text{with} \quad M_D(n,\theta) = \begin{cases} 1, & (n,\theta) \notin D \\ 0, & (n,\theta) \in D \end{cases}$$

where the mask $M_D(n,\theta)$ is zero in D and unity outside D. Given a real-valued TF model function $\widetilde{W}(n,\theta)$, the synthesized signal is now defined as the signal whose MWD is closest to the model[2]

$$x_{\text{opt}}(n) = \arg\min_x \epsilon_x^{(D)} \tag{2}$$

where

$$\epsilon_x^{(D)\,2} = \left\|\widetilde{W} - W_x^{(D)}\right\|^2 = \sum_n \int_{-1/4}^{1/4} \left[\widetilde{W}(n,\theta) - W_x^{(D)}(n,\theta)\right]^2 d\theta.$$

[2] Signal synthesis using a masked *cross-WD* with a fixed reference signal has been proposed in [9]. This problem leads to linear, generally ill-conditioned equations. In contrast, our method uses a masked *auto-WD*, which avoids the use of a reference signal but will be seen to lead to third-order equations.

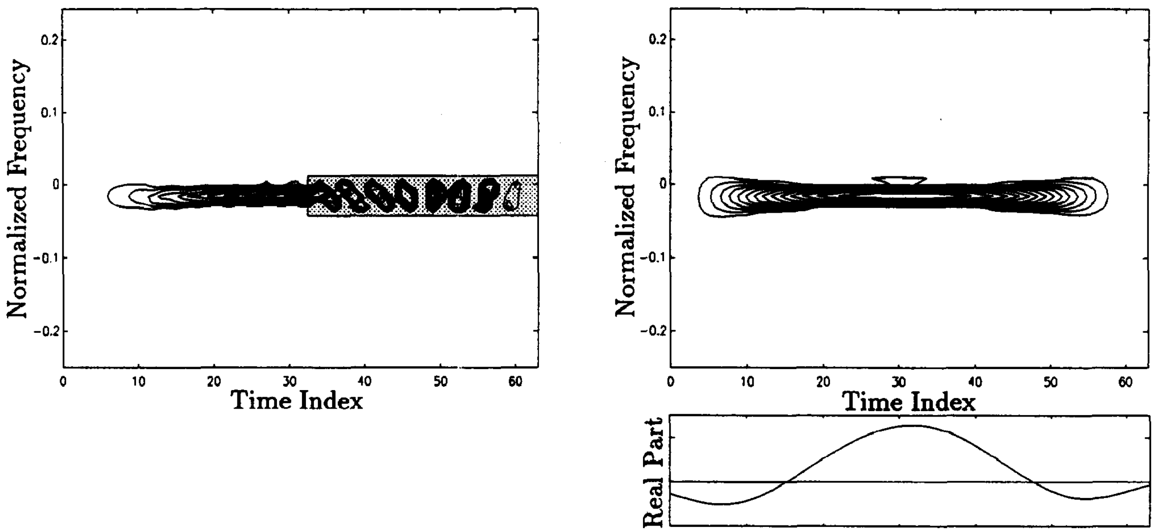

(a) (b)

Fig. 2. Application of MWD-based signal synthesis to the signal separation problem considered in Fig. 1: (a) TF model function (cf. Fig. 1(c)) and don't-care region (shaded) containing the IT; (b) result of MWD-based synthesis. Note that the IT does not influence the synthesis result and that the signal is correctly synthesized in the don't-care region.

We emphasize that MWD-based signal synthesis reduces to conventional signal synthesis for a mask $M_D(n,\theta) \equiv 1$. Splitting up the synthesis error to be minimized as

$$\epsilon_x^{(D)\,2} = \sum_{(n,\theta)\notin D} \int \left[\widetilde{W}(n,\theta) - W_x(n,\theta)\right]^2 d\theta + \sum_{(n,\theta)\in D} \int \left[\widetilde{W}(n,\theta)\right]^2 d\theta \qquad (3)$$

(where we have used the fact that $W_x^{(D)}(n,\theta) = W_x(n,\theta)$ for $(n,\theta) \notin D$ and $W_x^{(D)}(n,\theta) = 0$ for $(n,\theta) \in D$), we see that the signal $x(n)$ depends (via its WD) exclusively on those parts of the model $\widetilde{W}(n,\theta)$ that are *outside* D. In fact, the region D is recognized as a *don't-care region* where the model does not influence the synthesis result. The result of MWD-based synthesis for the example considered in Fig. 1 is shown in Fig. 2. We see that the synthesized signal is very close to the true signal component.

It is instructive to compare this result to the result of conventional signal synthesis where the parasitic IT's are masked out, i.e., the mask $M_D(n,\theta)$ is applied to the *model* instead of the WD. Here, the synthesis error to be minimized is

$$\epsilon_x^2 = \sum_n \int_{-1/4}^{1/4} \left[\widetilde{W}(n,\theta)\, M_D(n,\theta) - W_x(n,\theta)\right]^2 d\theta$$
$$= \sum_{(n,\theta)\notin D} \int \left[\widetilde{W}(n,\theta) - W_x(n,\theta)\right]^2 d\theta + \sum_{(n,\theta)\in D} \int [W_x(n,\theta)]^2 d\theta .$$

Although the first error term is as in (3), the second error term now depends on the signal $x(n)$ in such a way that signal components inside D are penalized; hence, the signal will ideally be set to zero in D, which causes an undesired truncation of the signal. This is verified by computer simulation (see Fig. 3).

II. The Quasi Power Algorithm

In this section, we propose an iterative algorithm for MWD-based signal synthesis. In order to solve the minimization problem (2), we first note that the MWD can be written as

$$W_x^{(D)}(n,\theta) = 2 \sum_m c_x^{(D)}(n,m)\, e^{-j4\pi\theta m}$$
$$\text{with} \quad c_x^{(D)}(n,m) = \sum_{m'} \mu_D(n, m-m')\, c_x(n,m')$$

where $c_x(n,m) = x(n+m)\, x^*(n-m)$ as before and $\mu_D(n,m) = 2\int_{-1/4}^{1/4} M_D(n,\theta)\, e^{j4\pi\theta m}\, d\theta$. Using Parseval's theorem, the synthesis error can be reformulated as

$$\epsilon_x^{(D)\,2} = \left\|\widetilde{W} - W_x^{(D)}\right\|^2 = 2\left\|\tilde{c} - c_x^{(D)}\right\|^2$$
$$= 2 \sum_n \sum_m \left|\tilde{c}(n,m) - c_x^{(D)}(n,m)\right|^2,$$

where $\tilde{c}(n,m) = \int_{-1/4}^{1/4} \widetilde{W}(n,\theta)\, e^{j4\pi\theta m}\, d\theta$. Setting the derivatives of $\epsilon_x^{(D)\,2}$ with respect to the signal samples $x(n)$ equal to zero yields the following necessary condition for minimum $\epsilon_x^{(D)}$:

$$\sum_{n'} x(2n'-n)\, C_x(n', n-n') = 0 \qquad \forall\, n \qquad (4)$$

with

$$C_x(n,m) = \sum_{m'} \mu_D^*(n, m'-m)\left[\tilde{c}(n,m') - c_x^{(D)}(n,m')\right].$$

Separating these equations into a subset for even n ($n = 2k$) and a subset for odd n ($n = 2k+1$) yields[3]

$$\boldsymbol{Q}'_{e,x}\, \boldsymbol{x}_e = \boldsymbol{0}\,, \qquad \boldsymbol{Q}'_{o,x}\, \boldsymbol{x}_o = \boldsymbol{0} \qquad (5)$$

[3] Since both matrices $\boldsymbol{Q}'_{e,x}$ and $\boldsymbol{Q}'_{o,x}$ generally contain all signal samples $x(n)$, (5) does not imply that even-indexed and odd-indexed signal samples can be synthesized independently of each other.

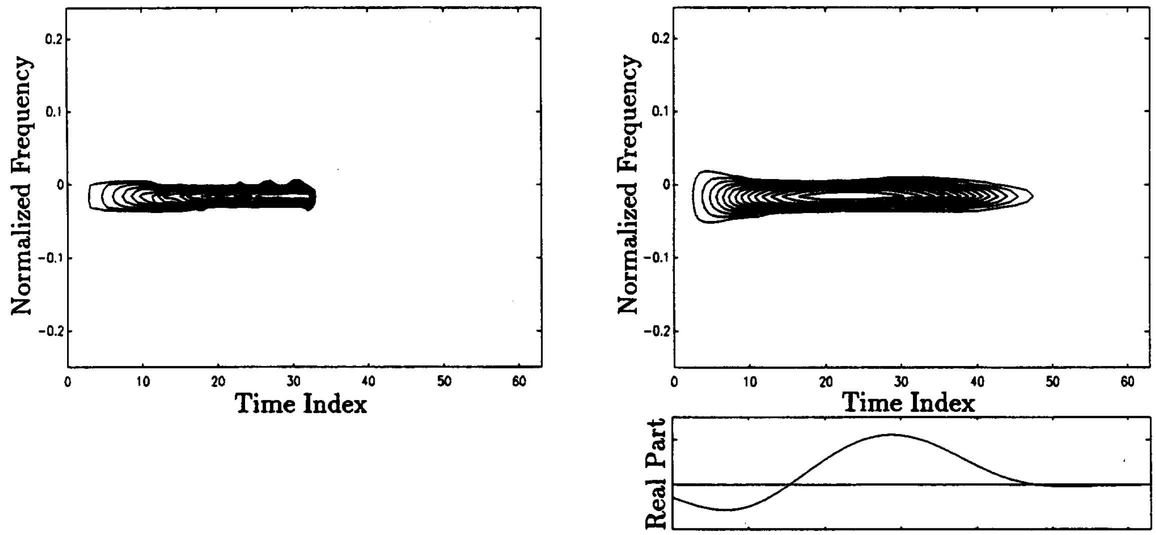

(a) (b)

Fig. 3. Application of conventional WD-based signal synthesis to a TF model where the IT is masked out: (a) TF model function; (b) result of WD-based synthesis (this should be compared with the result of MWD-based synthesis in Fig. 2(b)). The truncation of the model leads to an undesired truncation in the synthesized signal.

where the Hermitian matrices $Q'_{e,x}$ and $Q'_{o,x}$ are defined as

$$\left(Q'_{e,x}\right)_{kl} = C_x(k+l, k-l)\,, \quad \left(Q'_{o,x}\right)_{kl} = C_x(k+l+1, k-l)\,, \quad (6)$$

and x_e and x_o denote the vectors of even-indexed and odd-indexed signal samples $(x_e)_k = x(2k)$ and $(x_o)_k = x(2k+1)$, respectively.

The necessary condition (4) or, equivalently, (5) is a set of third-order equations that apparently do not allow a closed-form solution. An analogous set of equations is obtained for a similar problem, namely, signal synthesis based on a *smoothed* WD [8]. Proceeding like in that case, we adopt an iterative algorithm known as the *quasi power algorithm* (QPA), whose background is discussed in detail in [8]. The ith iteration of the QPA is as follows (see [10] for an efficient implementation):

1) Using the signal $x^{(i-1)}(n)$ calculated at the previous iteration, form the matrices

$$Q_{e,x^{(i-1)}} = Q'_{e,x^{(i-1)}} + x_e^{(i-1)}\, x_e^{(i-1)H}\,,$$
$$Q_{o,x^{(i-1)}} = Q'_{o,x^{(i-1)}} + x_o^{(i-1)}\, x_o^{(i-1)H}\,. \quad (7)$$

where $Q'_{e,x^{(i-1)}}$ and $Q'_{o,x^{(i-1)}}$ are defined in (6), and ^{H} denotes complex conjugate transposition.

2) Calculate $u_e^{(i)}$ and $\lambda_e^{(i)}$ as

$$v_e^{(i)} = Q_{e,x^{(i-1)}}\, u_e^{(i-1)}\,; \quad \lambda_e^{(i)} = \|v_e^{(i)}\|\,; \quad u_e^{(i)} = \frac{1}{\lambda_e^{(i)}} v_e^{(i)}$$

where $u_e^{(i-1)}$ is the result of the previous iteration. Use analogous operations to obtain $u_o^{(i)}$ and $\lambda_o^{(i)}$.

3) Form the signal $x^{(i)}(n)$ by interleaving even-indexed and odd-indexed signal samples

$$x^{(i)}(2k) = \sqrt{\lambda_e^{(i)}}\left(u_e^{(i)}\right)_k, \quad x^{(i)}(2k+1) = \sqrt{\lambda_o^{(i)}}\left(u_o^{(i)}\right)_k.$$

On convergence ($i \to \infty$), the synthesis result $x(n)$ is finally obtained as

$$x(2k) = e^{j\phi_e}\, x^{(\infty)}(2k)\,, \qquad x(2k+1) = e^{j\phi_o}\, x^{(\infty)}(2k+1)$$

where ϕ_e and ϕ_o are arbitrary constant phases that can be determined as discussed in [11].

Fig. 4 demonstrates the convergence of the QPA. The start signal $x^{(0)}(n)$ was chosen as a noise signal whose energy is irregularly spread over the TF plane. After convergence, the synthesis result has adapted to the model function while ignoring the model component inside the don't-care region. Note that a significant residual synthesis error naturally remains since the model component in the don't-care region is not matched by the synthesized signal.

The QPA has been observed in experiments to converge reliably, although a formal proof of convergence does not exist so far. In the case of convergence, the signal obtained is guaranteed to satisfy the necessary condition (4). The QPA reduces to the classical power algorithm [8] in the special case of WD-based synthesis (i.e., no don't-care region or $M_D(n,\theta) \equiv 1$). A good choice of the start signal used for initializing the QPA is a noise signal bandlimited to the WD's fundamental frequency interval (halfband) $-1/4 < \theta < 1/4$. (Other halfband locations can be accommodated as well, e.g., the halfband $0 < \theta < 1/2$ corresponding to analytic signals.) We note that MWD-based signal synthesis and the QPA can be extended to nonbinary (e.g., smooth) masks in a straightforward manner. Finally, halfband-constrained versions of the QPA (where the synthesis result is a halfband signal whose WD is nonaliased) have been proposed for smoothed WD's [6], [8], [10] and are readily adapted to the MWD.

III. Performance of MWD-Based Signal Synthesis

A. Time-Frequency Extrapolation

MWD-based signal synthesis possesses a "TF extrapolation capability," i.e., a capability of adequately synthesizing signal parts in the don't-care region where no model information is used. This capability depends on the availability of "indirect information" contained in the WD's IT's. Indeed, MWD-based signal synthesis is capable of restoring a signal component in the don't-care region D if there exists at least one other signal component that is outside D and whose IT with the signal component to be restored is outside D as well. This principle is illustrated in Fig. 5.

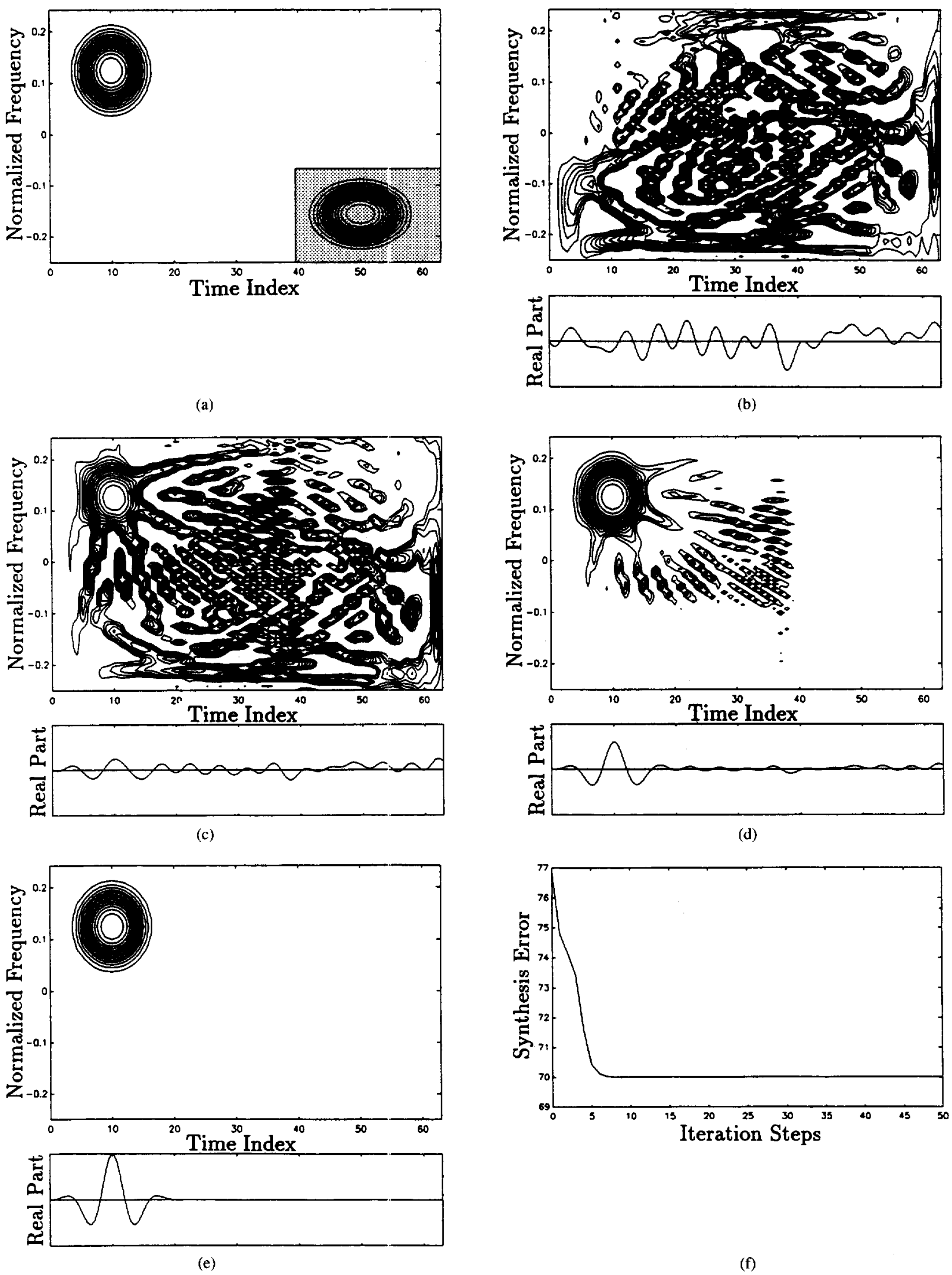

Fig. 4. Convergence of the QPA: (a) TF model function and don't-care region (shaded); (b) real part and WD of start signal $x^{(0)}(n)$; (c)-(e) real parts and WD's of iteration signals $x^{(i)}(n)$ for $i = 3$, 4, and 10, respectively; (f) synthesis error $\epsilon_x^{(D)}$ for the iteration signals $x^{(i)}(n)$ with $0 \leq i \leq 50$.

The TF extrapolation effect also occurs in the case of monocomponent signals. Here, the indirect information contained in the "inner IT's" [2] is utilized for extrapolation. From the geometry of inner IT's [2], it is possible to derive the rule of thumb that a signal is restored if at least one half of the signal's effective TF support lies outside the don't-care region D. An example is shown in Fig. 6. It is

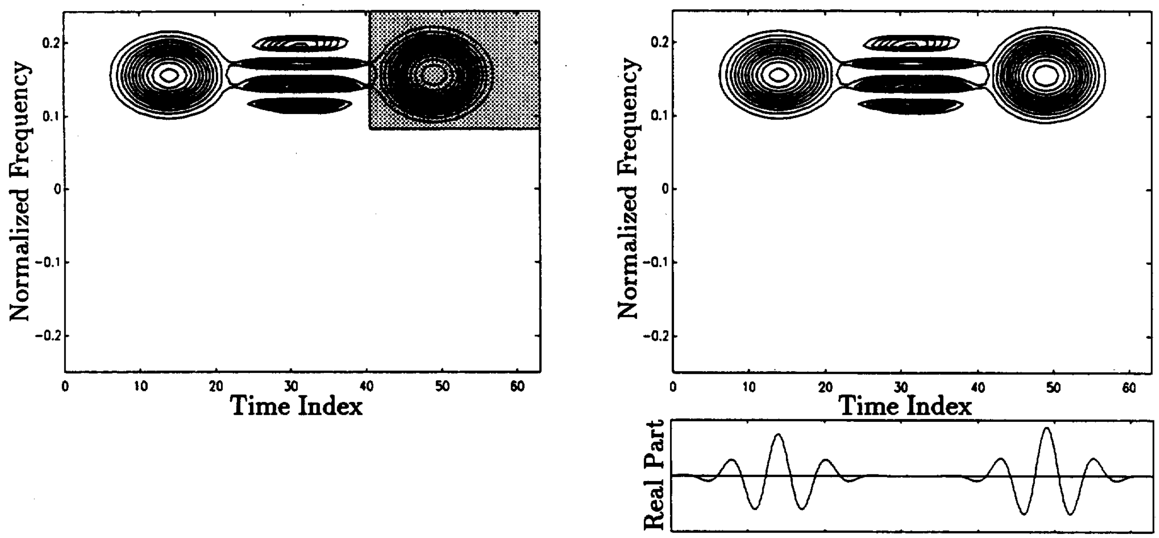

(a) (b)

Fig. 5. Restoration of a signal component located in the don't-care region: (a) TF model and don't-care region (shaded); (b) result of MWD-based signal synthesis. The information contained in the IT is used for correctly restoring the signal component in the don't-care region.

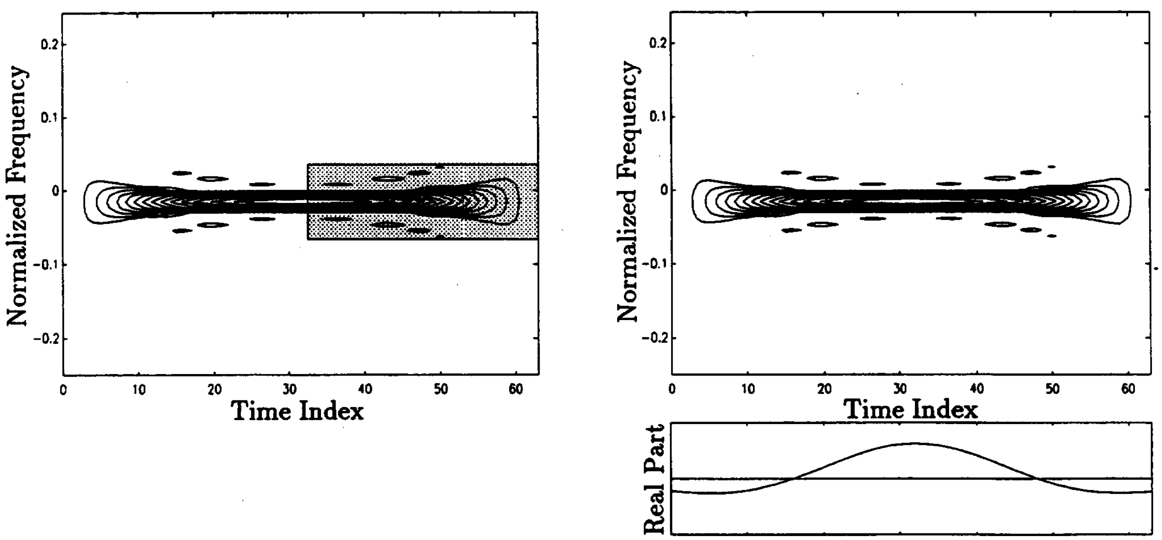

(a) (b)

Fig. 6. TF extrapolation of a monocomponent signal: (a) TF model and don't-care region (shaded); (b) result of MWD-based signal synthesis. The signal is correctly extrapolated since slightly more than one half of the signal's WD lies outside the don't-care region.

this extrapolation effect that resulted in the restoration of the desired signal component in Fig. 2.

B. Spurious Signal Components and Energy Penalty

If the don't-care region D is large and there is a lack of model parts outside D that indirectly specify the signal inside D, then the synthesized signal may contain *spurious signal components*. Indeed, it follows from (3) that the synthesis error is independent of the part of $W_x(n,\theta)$ located inside D. Thus, signal components inside D are not penalized *as long as they do not lead to an IT outside D*. This rule is illustrated in Fig. 7, which compares the results of MWD-based signal synthesis for a given model and various don't-care regions.

An effective and inexpensive way to avoid spurious signal components is based on the observation that although spurious signal components do not influence the synthesis error minimized, they do increase the total energy of the synthesized signal. Thus, we may augment the synthesis error $\epsilon_x^{(D)\,2}$ by an "energy penalty" and define the new error

$$\epsilon_x^{(D,\gamma)\,2} \triangleq \epsilon_x^{(D)\,2} + \gamma\,\|W_x\|^2 = \|\widetilde{W} - W_x^{(D)}\|^2 + \gamma\,\|W_x\|^2.$$

Here, $\gamma \geq 0$ is a parameter characterizing the relative weight of the energy penalty as compared with the "conventional" error component $\epsilon_x^{(D)\,2}$, and $\|W_x\|^2 = \sum_n \int_{-1/4}^{1/4} W_x^2(n,\theta)\,d\theta$ is the energy of the signal's WD.[4] Redoing all calculations using the energy-penalized error $\epsilon_x^{(D,\gamma)\,2}$ shows that the QPA remains valid with the only difference that the matrices $\boldsymbol{Q}_{\epsilon,x}$ and $\boldsymbol{Q}_{o,x}$ are formally replaced

[4] For halfband signals where $W_x(n,\theta)$ is nonaliased, $\|W_x\|^2 = E_x^2$ where $E_x = \sum_n |x(n)|^2$ is the signal's energy.

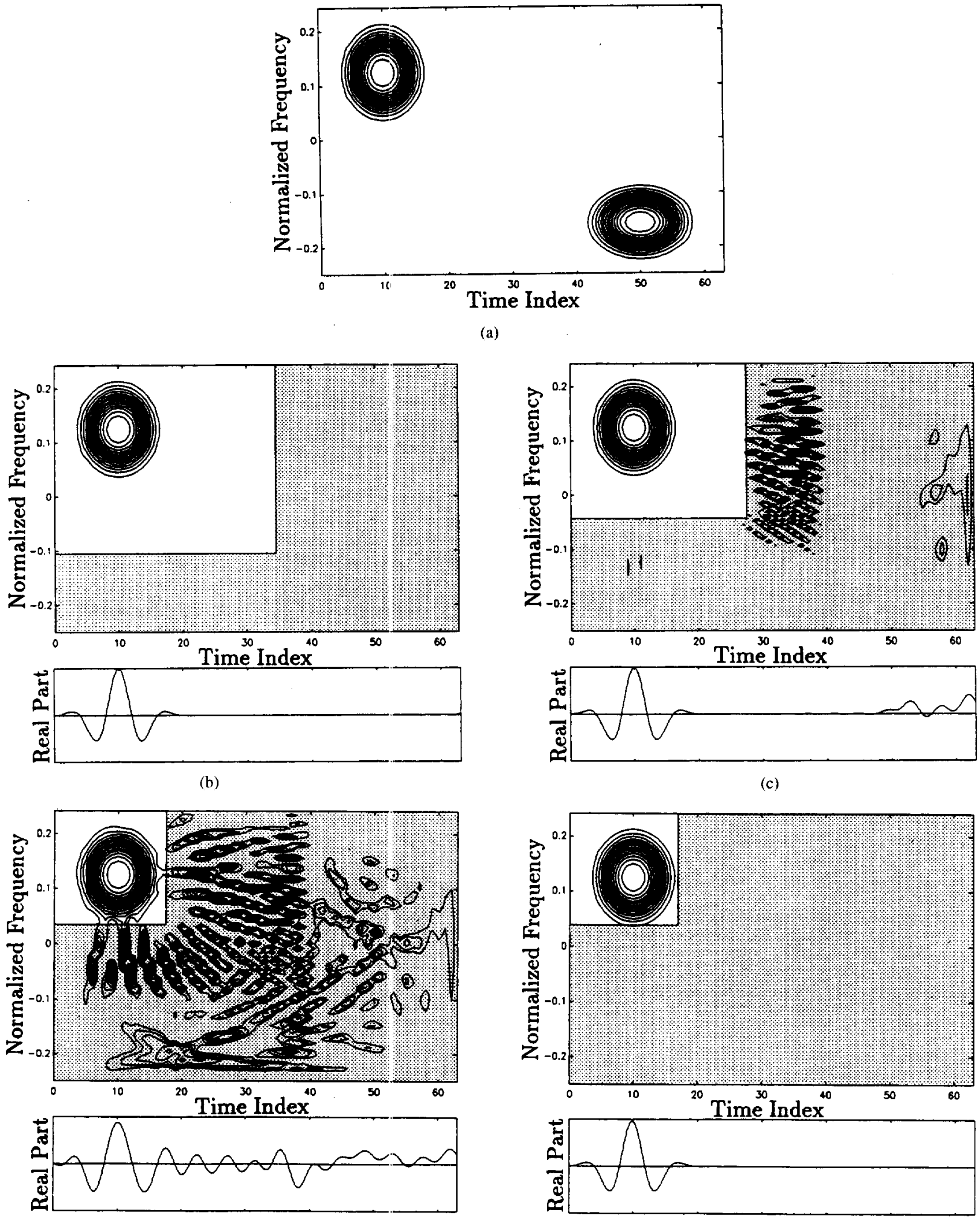

Fig. 7. Dependence of spurious signal components on the don't-care region and effect of energy penalty: (a) TF model; (b)-(d) results of MWD-based signal synthesis (without energy penalty) for various don't-care regions (shaded); (e) result of MWD-based signal synthesis with energy penalty ($\gamma = 0.01$). Fig. 7(e) should be compared with Fig. 7(d) showing the corresponding result obtained without energy penalty.

by (cf. (7))

$$Q_{e,x}^{(\gamma)} \triangleq Q_{e,x} - \gamma\, x_e x_e^H = Q'_{e,x} + (1-\gamma)\, x_e x_e^H$$
$$Q_{o,x}^{(\gamma)} \triangleq Q_{o,x} - \gamma\, x_o x_o^H = Q'_{o,x} + (1-\gamma)\, x_o x_o^H.$$

Fig. 7(e) shows that the energy penalty is capable of effectively suppressing spurious signal components. Note, however, that choosing the penalty factor γ too small or too large results in an incomplete suppression of spurious signal components or a downscaling of the signal, respectively.

IV. Conclusion

MWD-based signal synthesis is an effective method for time-frequency signal synthesis with insensitivity to model corruptions located in known time-frequency regions. The third-order equations resulting from this approach can be solved by a version of the quasi power algorithm previously proposed for smoothed WD's. MWD-based signal synthesis was shown to possess a desirable time-frequency extrapolation capability. The occurrence of spurious signal components in the don't-care regions is easily avoided through the inclusion of an energy penalty in the synthesis error.

References

[1] T. A. C. M. Claasen and W. F. G. Mecklenbräuker, "The Wigner distribution—A tool for time-frequency signal analysis, Parts I–III," *Philips J. Res.*, vol. 35, pp. 217–250; 276–300; 372–389, 1980.

[2] F. Hlawatsch and P. Flandrin, "The interference structure of the Wigner distribution and related time-frequency signal representations," to appear in *The Wigner Distribution—Theory and Applications in Signal Processing* (W. Mecklenbräuker, Ed.). Amsterdam: Elsevier, 1994.

[3] F. Hlawatsch and G.F. Boudreaux-Bartels, "Linear and quadratic time-frequency signal representations," *IEEE Signal Processing Mag.*, vol. 9, no. 2, pp. 21–67, Apr. 1992.

[4] G.F. Boudreaux-Bartels and T.W. Parks, "Time-varying filtering and signal estimation using Wigner distribution synthesis techniques," *IEEE Trans. Acoust., Speech, Signal Processing*, vol. ASSP-34, pp. 442–451, June 1986.

[5] F. Hlawatsch and W. Krattenthaler, "Bilinear signal synthesis," *IEEE Trans. Signal Processing*, vol. 40, no. 2, pp. 352–363, Feb. 1992.

[6] ——, "Signal synthesis algorithms for bilinear time-frequency signal representations," to appear in *The Wigner Distribution—Theory and Applications in Signal Processing* (W. Mecklenbräuker, Ed.). Amsterdam: Elsevier, 1994.

[7] G. F. Boudreaux-Bartels, "Time-varying signal processing using Wigner distribution synthesis techniques," to appear in *The Wigner Distribution—Theory and Applications in Signal Processing* (W. Mecklenbräuker, Ed.). Amsterdam: Elsevier, 1994.

[8] W. Krattenthaler and F. Hlawatsch, "Time-frequency design and processing of signals via smoothed Wigner distributions," *IEEE Trans. Signal Processing*, vol. 41, no. 1, pp. 278–287, Jan. 1993.

[9] T. J. McHale and G. F. Boudreaux-Bartels, "An algorithm for synthesizing signals from partial time-frequency models using the cross Wigner distribution," *IEEE Trans. Signal Processing*, vol. 41, no. 5, pp. 1986-1990, May 1993.

[10] W. Krattenthaler, "Signal synthesis algorithms for non-smoothed and smoothed Wigner distributions," Doctoral dissertation, Technische Universität Wien, Vienna, Austria, 1990.

[11] F. Hlawatsch and W. Krattenthaler, "Phase matching algorithms for Wigner distribution signal synthesis," *IEEE Trans. Signal Processing*, vol. 39, no. 3, pp. 612-619, Mar. 1991.

Second-Order Statistical Analysis of Totally Weighted Subspace Fitting Methods

Ridha Hamza and Kevin Buckley

***Abstract*—In this correspondence, we analyze the effects of a limited number of snapshots on a general class of multidimensional signal subspace estimation methods, termed totally weighted subspace fitting (TWSF) methods. This class is an extension of the weighted subspace fitting technique that includes row weighting and column weighting of the signal subspace matrix. We quantify the asymptotic statistical properties of the TWSF method by means of a second-order statistical analysis. The main contribution of this correspondence is that it provides, for the first time, the estimator bias. Some simulation results are included to validate our analytical results.**

I. Introduction

The development of the weighted subspace fitting (WSF) formulation for sensor array processing has unified many popular multidimensional signal subspace methods under a common framework [1]. Some of the established algorithms that belong to this class are classical beamforming, deterministic maximum likelihood (ML), and multidimensional (MD)-MUSIC. Extension of the WSF method to include other classes of source localization methods, such as ESPRIT [7], has been made possible by means of row weighting [1].

This correspondence formulates all the above methods in a more general class, termed totally weighted subspace fitting (TWSF). The unified class incorporates column weighting, advocated by Viberg and Ottersten [1], and row weighting, which can consist of structural weighting [1] or focusing weighting [7].

A lot of studies are restricted to the first-order statistical analysis that yields to zero estimate error bias. However, simulation results indicate that bias can be significant for some cases. Thus, bias is an important performance characteristic. To date, no bias analysis has been presented on TWSF methods. Recently, Xu and Buckley [3] have analyzed the general class of eigenspace spectrum methods. They derived concise expressions for the variance and bias. Our contribution here is to extend the analytical approach in [3] to the totally weighted subspace fitting algorithm class.

II. TWSF Method Framework

Assume a linear array of M sensors and D narrow-band noncoherent far-field emitters impinging on the array ($D < M$). Define $\vec{a}(\theta) \in \mathcal{C}^M$ to be the steering vector at DOA θ. The collection of these vectors $\mathcal{A}$ over the *field-of-view* Θ_{fov} is termed the *array manifold.* $\mathcal{A}$ is assumed to be known and unambiguous, i.e., any collection of $D+1$ direction vectors is linearly independent. Let

$$\mathcal{A}^D = \{A/A = [\vec{a}(\theta_1), \ldots, \vec{a}(\theta_D)]; \theta_i's \in \Theta_{\text{fov}} \;\&\; \theta_i \neq \theta_j\}. \quad (1)$$

Consider the standard model of an array observation. The spatial correlation matrix is thus given by

$$R_{zz} = AP_sA^H + \sigma_n^2 I_M \quad (2)$$

Manuscript received October 9, 1992; revised December 17, 1993. This work was supported by ONR under contract no. N00014-90-J-1049. The associate editor coordinating the review of this paper and approving it for publication was Prof. Georgios B. Giannakis.

The authors are with the Department of Electrical Engineering, University of Minnesota, Minneapolis, MN 55455 USA.

IEEE Log Number 9403285.

1053-587X/94$04.00 © 1994 IEEE